FUDMA Journal of Renewable and Atomic Energy (FJoRAE)
ISSN: 3027-2335
Vol. 3 (SI) 2026 Pp 49-63
DOI: https://doi.org/10.33003/fjorae.2026.03SI.82

Defect Engineering Strategies for High-Performance Tin-Based Perovskite Solar Cells: Interface Defect Analysis of Hole and Electron Transport Layers Using SCAPS-1D Simulation

Dahiru M. Sanni[1]*, Bashir Ahuome Abubakar[1] and Aniefiok Francis Akpaneno[2]

[1]Department of Physics, Federal University Dutsin-Ma, P.M.B. 5001, Dutsin-Ma, Katsina State, Nigeria
[2]Department of Geophysics, Federal University Dutsin-Ma, P.M.B. 5001, Dutsin-Ma, Katsina State, Nigeria

*Corresponding Author's e-mail: dahirusanni@gmail.com

ABSTRACT
Tin-based perovskite solar cells (TPSCs) are emerging as attractive lead-free alternatives to conventional lead-based perovskite solar cells due to their low toxicity, good carrier mobility, small bandgap, and great optical absorption. However, the existence of bulk and interfacial imperfections severely limits the photovoltaic performance and long-term stability of TPSCs. Here, SCAPS-1D simulation was used to systematically design defects and study the densities of interfacial defects between the absorber layer and several hole transports layers (HTLs) such as CuI, $CuAlO_2$, $CuSbS_2$, MoS_2, CuO and Cu_2O. The photovoltaic properties of FTO/WS_2/$MASnI_3$/HTL/Au device designs were thoroughly studied under the influence of interface defect density in the range of 10^{12} to 10^{20} cm^{-3}. In addition, the effects of the defect density of the absorber layer and the defects of the ETL/absorber interface were also studied. The results demonstrate that $CuSbS_2$ and $CuAlO_2$ have better defect tolerance with maximum power conversion efficiencies (PCEs) of 24.16% and 22.83%, respectively, while CuO and CuI show severe performance loss at high defect densities. The $CuSbS_2$ and $CuAlO_2$-based devices showed exceptional stability against changes in interface defects, implying enhanced interfacial charge extraction and lower non-radiative recombination losses. From the absorber defect analysis, it was shown that the increase in the bulk defect density has a severe impact on open circuit voltage, (Voc) fill factor (FF) and power conversion efficiency (PCE) which is suppressed due to Shockley-Read-Hall recombination. The results emphasize the importance of interface engineering and the choice of suitable transport layers for enhancing the efficiency and stability of lead-free TPSCs.

Keywords: Tin-based perovskite solar cells, SCAPS-1D, Interface defects, Defect engineering, Hole transport layer, $CuSbS_2$, $CuAlO_2$, Lead-free perovskites

1.0. INTRODUCTION

Perovskite solar cells (PSCs) have received a great deal of attention from the photovoltaic research community owing to their remarkable optoelectronic properties, low fabrication cost, tunable bandgap and rapidly increasing power conversion efficiencies (PCEs) (Kim et al., 2012; Lee et al., 2012; Stranks et al., 2013). Lead-based PSCs have reached verified efficiency of over 26% (National Renewable Energy Laboratory (NREL), 2025). However, the toxicity of lead is a critical environmental problem that limits their widespread commercialization. Therefore, eco-friendly alternatives to next-generation photovoltaic technologies have been developed through the development of lead-free perovskite materials, especially tin-based

perovskites. Due to their high absorption coefficients, small bandgaps, long carrier diffusion lengths and strong charge carrier mobility, tin (Sn)-based perovskites (TPSCs) are attractive (Li et al., 2023; S. Wang & Xiu, 2025; X. Wang et al., 2024).

Recent researches have shown significant development in TPSCs via compositional optimization, additive engineering, and interface passivation approaches (S. Wang & Xiu, 2025; Zhang et al., 2025). However, the efficiency and operational stability of TPSCs are worse than lead-based PSCs, mainly due to the fast oxidation of Sn^{2+} to Sn^{4+}, high concentration of self-doping and defect-assisted recombination losses (Zhang et al., 2025). Interface defects at the interfaces between the absorber layer (AL) and charge transport layers (CTLs) are very important for the device performance, because they influence charge extraction, carrier recombination and energy band alignment.

Thus, defect engineering has been considered as an effective technique for improving the efficiency and stability of TPSCs. Previous investigations have demonstrated that the optimal interface passivation can reduce the non-radiative recombination, increase the carrier lifetime and boost the open-circuit voltage (Sharma, V. et al., 2018; Sherkar et al., n.d.). Alongside absorber engineering, appropriate CTLs are needed. Tungsten disulfide (WS_2) has emerged as a promising ETL: it has excellent electron mobility and alignment with Sn-perovskite conduction bands (Asif et al., 2025). On the HTL side, inorganic oxides and chalcogenides (CuI, Cu_2O, $CuAlO_2$, MoS_2, CuO, $CuSbS_2$, etc.) are attractive due to thermal stability and abundant composition. For example, CuI has high p-type conductivity and wide bandgap, and was recently demonstrated as an effective HTL in TPSCs, yielding 20% efficiency (Pau et al., 2025). $CuAlO_2$ and related oxides have also been simulated as HTLs with ~19.8% PCE (Shasti, M. and Mortezaali, 2019). Given the proliferation of novel materials, their comparative study in tin PSCs is needed.

Despite experimental progress, comprehensive simulation studies are scarce. Solar Cell Capacitance Simulator (SCAPS-1D) is widely used for device modeling, solving the Poisson and continuity equations for all layers (Bhujbal et al., 2024). Previous simulations on lead-free PSCs highlight the dominance of defect densities on performance: for example, Islam et al. found that WS_2-ETL devices reached 32.3% PCE in ideal tin-halide cells when defect densities were minimized (Islam et al., 2026). Sobayel et al. used SCAPS to show that absorber defect densities above ~10^{15} cm^{-3} degrade $CH_3NH_3PbI_3$ cell PCE drastically (Sobayel et al., 2019). However, detailed studies focusing on WS_2 ETL with Sn-perovskite absorber, and comparing multiple HTLs under varying defect conditions, are lacking.

This work aims to fill this gap by systematically simulating a FTO/WS_2/Sn-perovskite/HTL/Au architecture. We vary AL thickness, doping, mobility and sweep defect densities at interfaces and in the bulk, for each candidate HTL. The objectives are (1) to quantify how defect densities affect Voc, Jsc, FF, and PCE; (2) to identify the best-performing HTL among CuI, MoS_2, $CuAlO_2$, CuO, $CuSbS_2$, and Cu_2O; and (3) to interpret results via energy band alignment and recombination physics. All claims are supported by recent studies (Islam et al., 2026; Javed et al., 2024; Pau et al., 2025; Sobayel et al., 2019). This analysis will provide design guidelines (defect tolerance thresholds, optimal materials) for future high-efficiency TPSCs.

2.0. MATERIALS AND METHOD

2.1. Device Architecture

The simulated solar cell topologies were composed of fluorine-doped tin oxide (FTO) as the front contact, WS_2 as the electron transport layer (ETL), tin-based perovskite as the absorber layer, different HTLs (MoS_2, $CuSbS_2$, CuO, Cu_2O, $CuAlO_2$, and CuI), and Au as the rear metal contact. The examined device configurations and the energy band diagram are presented in Figure 1.

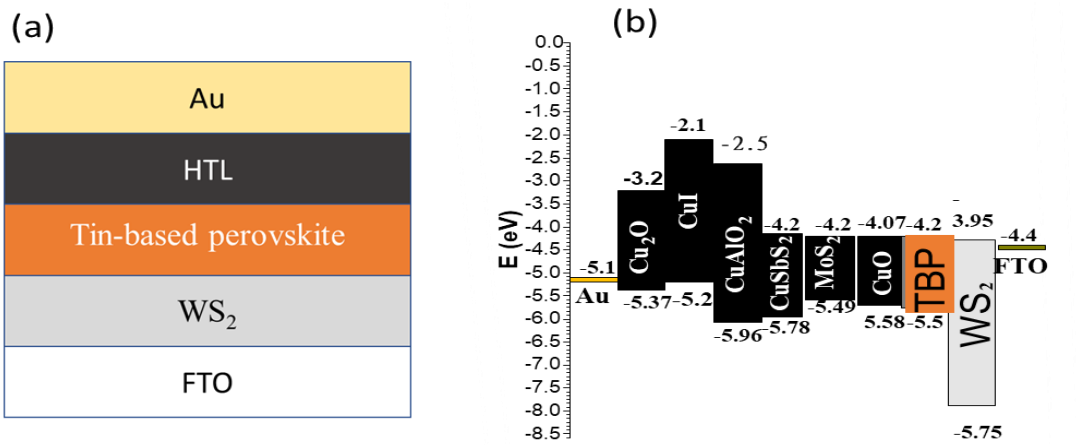

Figure 1: (a) Perovskite solar cell structure (bO Energy band diagram

All numerical calculations were performed using the Solar Cell Capacitance Simulator (SCAPS-1D) program under the conventional AM1.5G illumination at a 1000 W/m^2 and 300 K. The basic equations for the SCAPS-1D are Poisson equation, drift diffusion, and the continuity equations governing the electrons and holes behaviour were used for the simulation (Rachidy C. et al., 2021)

$$\frac{d^2\phi(x)}{dx^2} = \frac{q}{\varepsilon_o \varepsilon_r}\left(p(x) - n(x) + N_D - N_A + \rho_p - \rho_n\right) \quad (1)$$

$$\frac{\partial n}{\partial t} = -\frac{\partial}{\partial x}J_n - U_n + G \quad (2)$$

$$\frac{\partial p}{\partial t} = -\frac{\partial}{\partial x}J_p - U_n + G$$

$$J_p = +\frac{\mu_p P}{q}\frac{\partial E_{FP}}{\partial x}, \quad (3)$$

$$J_n = -\frac{\mu_p n}{q}\frac{\partial E_{Fn}}{\partial x}$$

Where the symbols ε_0 and ε_r are the vacuum dielectric constant and the relative dielectric constant, respectively. The n and p represent the concentration of free carriers for electrons and holes, respectively. N_D is the concentration of donor impurity, and N_A represents the acceptor impurity. The charge densities of electrons and holes are denoted by ρ_n and ρ_p, respectively, $\boldsymbol{\phi}$ represents the electric field, and q is the electrical charge, with a typical value of around 1.602 10^{-19} C. U_n and G represent recombination rate and carrier generation, J_n *and* J_p are the current densities for electrons and holes respectively, μ_p *and* μ_n are the hole and electron mobility, respectively, E_{FP} and E_{FP} are Fermi levels of electron and hole mobility.

2.2. Interface Defect Simulation

The effect of the interface defects was studied by varying the defect density at the AL/HTL interface and AL/ETL interface from 10^{12} to 10^{20} cm^{-3}. The photovoltaic metrics studied were open-circuit voltage (Voc), short-circuit current density (Jsc), fill factor (FF), and power conversion efficiency (PCE). The defect density fluctuation was investigated using the Shockley–Read–Hall (SRH) recombination theory, stating that increased defect densities lead to more trap-assisted recombination, thus decreasing carrier lifespan and extraction efficiency.

2.3. Bulk Defect Density Analysis

The defect density of the absorber layer was also adjusted from 10^{15} to 10^{20} cm^{-3} in order to study the influence of bulk recombination on the device performance. The investigation provides an insight into the defect tolerance of the tin-based absorber material. All the numerical calculations were performed using the Solar Cell Capacitance Simulator (SCAPS-1D) software under conventional AM1.5G illumination of 1000 W/m^2 at 300 K.

Table 1: Parameters of the absorber layer, different HTLs and WS_2 (Asif et al., 2025; Atem & Makableh, 2025; Bhujbal et al., 2024; Islam et al., 2026; Mortadi et al., 2024; Obi et al., 2021)

Parameter	FTO	$MASnI_3$	CuO	$CuAlO_2$	MoS_2	$CuSbS_2$	Cu_2O	WS_2
Thickness (nm)	300	200–800	200	200	200	200	200	100
Band gap (eV)	3.50	1.3	1.51	3.46	1.29	1.58	2.17	1.8
Electron affinity (eV)	3.30	4.2	4.07	2.50	4.20	4.20	3.20	3.95
Dielectric permittivity	9.0	8.2	18.1	60.0	8.9	14.6	10.7	13.6
Conduction band DOS (cm^{-3})	2.2×10^{18}	1.0×10^{18}	2.2×10^{19}	2.0×10^{20}	2.2×10^{18}	2.0×10^{18}	2.0×10^{17}	1.00×10^{18}
Valence band DOS (cm^{-3})	1.8×10^{19}	1.0×10^{18}	5.5×10^{20}	1.8×10^{20}	1.8×10^{19}	1.0×10^{18}	1.1×10^{19}	2.40×10^{18}
Electron mobility ($cm^2{\cdot}V^{-1}{\cdot}s^{-1}$)	2.0×10^{3}	1.6	100	2	100	49	200	100
Hole mobility ($cm^2{\cdot}V^{-1}{\cdot}s^{-1}$)	1.0×10^{2}	1.6	0.1	8.6	150	49	80	100
Donor concentration (cm^{-3})	2.0×10^{19}	0	0	0	0	0	0	1.00×10^{18}
Acceptor concentration (cm^{-3})	0	3.2×10^{15}	1.0×10^{16}	1.0×10^{19}	1.0×10^{17}	1.0×10^{19}	1.0×10^{18}	0
Defect density Nt (cm^{-3})	1.0×10^{14}	1.0×10^{14}	1.0×10^{14}	1.0×10^{14}	1.0×10^{14}	1.0×10^{14}	1.0×10^{14}	1.00×10^{15}

Table 2: Parameter for the contacts

Contacts	Anode properties	Cathode properties
Metal work function(eV)	5.1	4.4
Surface recombination velocity of electrons (cm/s)	1.0×10^7	1.0×10^7
Surface recombination velocity of holes (cm/s)	1.0×10^7	1.0×10^7

Table 3: Electric properties of defects in the materials (He et al., 2021; Rachidy C. et al., 2021)

Parameter	Absorber	ETL	HTL
Defect type	Neutral	Single donor	Single donor
Capture cross section for electrons (cm^{-2})	1.0×10^{-15}	1.0×10^{-13}	1.0×10^{-14}
Capture cross section for holes (cm^{-2})	1.0×10^{-15}	1.0×10^{-14}	1.0×10^{-13}
Energetic distribution	Gauss	Gauss	Gauss
Energy level with respect to E_v	0.6 (above E_v)	1.2 (above E_v)	0.65 (above E_v)
Defect density ($1/cm^3$)	1×10^{15}	1×10^{15}	1×10^{15}

Table 4: Electric properties of defects at the interfaces (He et al., 2021; Rachidy C. et al., 2021)

Parameter	ETL/Absorber	Absorber/HTL
Defect type	Neutral	Neutral
Capture cross section for electrons (cm^{-2})	1.0×10^{-19}	1.0×10^{-19}
Capture cross section for holes (cm/s)	1.0×10^{-19}	1.0×10^{-19}
Energetic distribution	Single	Single
Energy level with respect to E_v	0.6	0.6
Characteristic energy (eV)	0.1	0.1
Interface defect density (cm^{-2})	1.0×10^{14}	1.0×10^{12} - 1.0×10^{20}

3.0. RESULTS AND DISCUSSION

3.1 Effect of Absorber/HTL Interface Defect Density for MoS_2 HTL

Table 5 and Figure 2 show the effect of absorber/MoS_2 interface defect density on the photovoltaic performance of the FTO/WS_2/$MASnI_3$//MoS_2/Au device. The results show that the photovoltaic parameters are strongly dependent on the interface defect density. The device showed a Voc of 1.011 V, Jsc of 27.24 mA/cm^2, FF of 84.88% and PCE of 23.38% with a low defect density of 10^{12} cm^{-3}

When the interface defect density grew to 10^{20} cm^{-3}, the efficiency was significantly reduced to 14.39%. The performance drops mostly because of the increase of trap-assisted recombination at the absorber/HTL interface, which impedes the extraction of carriers and increases the non-radiative losses. In the Shockley–Read–Hall (SRH) recombination theory, large defect concentrations induce trap states in the bandgap that serve as recombination foci for photogenerated carriers, which in turn reduces the carrier lifespan and diffusion length. Similar observations have been documented in tin-based and lead-based PSCs where interface imperfections have a considerable effect on Voc and FF degradation.

The dramatic decrease in Voc from 1.011 V to 0.744 V is further evidence of the important role played by recombination mechanisms in the device performance. The correlation between Voc reduction and rising interface defects has been linked to increased non-radiative recombination losses and decreased quasi-Fermi level splitting in perovskite solar cells (Javed et al., 2024; Sobayel et al., 2019). In addition, the decrease of Jsc at high defect density suggests the existence of interface traps that block the effective hole transport over the MoS_2/$MASnI_3$ interface. Previous studies have demonstrated that MoS_2 can enable effective charge extraction because of its layered structure and high carrier mobility (Ain et al., 2020; D et al., 2025). However, poor interface quality may lead to significant degradation of the device performance. The reduction of FF with higher defect density also implies increased carrier dispersion and transport barrier due to defect-induced charge entrapment. The results show that MoS_2 has a moderate defect tolerance, but requires the appropriate interface passivation for steady high-performance operation.

Table 5: FTO/WS_2/$MASnI_3$/MoS_2/Au

S/N	AL /HTL Interface defect density (cm^{-2})	Voc (V)	Jsc (mA/cm^2)	FF (%)	PCE (%)
1	10^{12}	1.011	27.24	84.88	23.38
2	10^{14}	0.866	27.23	85.87	20.24
3	10^{16}	0.762	26.34	80.63	16.20
4	10^{18}	0.745	23.51	82.31	14.41
5	10^{20}	0.744	23.44	82.44	14.39

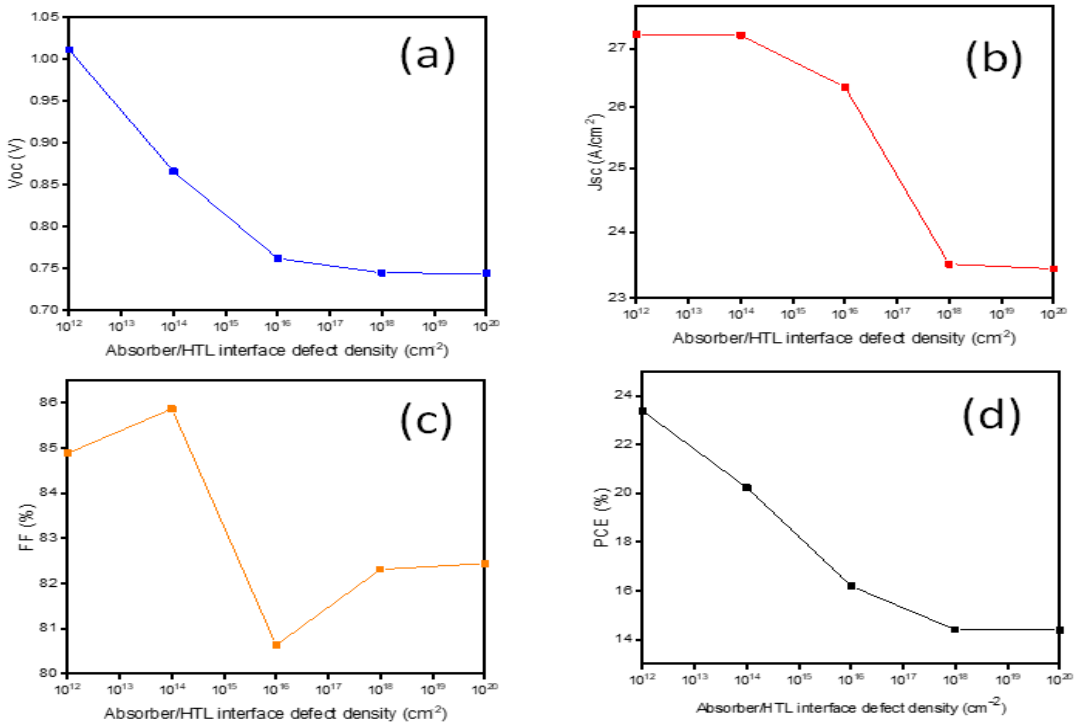

Figure 2: Absorber/ MoS_2 interfacial defect density

3.2. Effect of Absorber/$CuSbS_2$ Interface Defect Density

Table 6 and Figure 3 describe the performance metrics of the FTO/WS_2/$MASnI_3$/$CuSbS_2$/Au design. $CuSbS_2$ was shown to have the highest efficiency and the second-best defect tolerance among all the studied HTLs. For interface defect density of 10^{12} cm^{-3}, Voc of 1.142 V, Jsc of 24.90 mA/cm^2, FF of 84.95%, PCE of 24.16% were obtained. Interestingly, the efficiency only dropped marginally to 21.80% with interface defect density raised to 10^{20} cm^{-3} which translate to about 10% decrease in the PCE across the range of the defect densities. Such a modest degradation suggests a very good interface compatibility between the $MASnI_3$ absorber and $CuSbS_2$ HTL. The enhanced defect tolerance is attributable to the advantageous energy band alignment, increased hole mobility and reduced interface recombination velocity. This work has proven that valence band engineering of inorganic HTLs is a successful strategy to improve hole extraction and avoid electron back-transfer and recombination.

Also, at all defect densities, high fill factor values above 84% show effective charge extraction and low series resistance. The small fall in Voc with increasing defect density indicates that $CuSbS_2$ is more effective in suppressing recombination losses than other HTLs. This phenomenon can also be ascribed to the decreased interface state density and better charge selectivity. The better performance of $CuSbS_2$ can be ascribed to its small bandgap, high absorption coefficient and exceptional chemical stability. Previous studies have shown that $CuSbS_2$ possesses promising optoelectronic properties for photovoltaic applications, including favorable charge-carrier transport characteristics, high absorption coefficients, and defect-tolerant electronic behavior that can suppress non-radiative recombination losses (Chalapathi et al., 2024; Willian et al., 2016). Moreover, the lower sensitivity of the photovoltaic parameters to the defect density implies that $CuSbS_2$ is able to efficiently suppress trap-assisted recombination pathways. Thus, the findings indicate that $CuSbS_2$ is a very attractive inorganic HTL option for efficient and stable lead-free TPSCs.

Table 6: FTO/WS2/MASnI$_3$/CuSbS2/Au

S/N	HTL/Absorber Interface defect density (cm^{-2})	Voc(V)	Jsc (A/cm^2)	FF (%)	PCE (%)
1	10^{12}	1.142	24.90	84.95	24.16
2	10^{14}	1.141	24.89	85.04	24.15
3	10^{16}	1.100	24.69	86.47	23.50
4	10^{18}	1.066	23.54	87.06	21.85
5	10^{20}	1.065	23.49	87.11	21.80

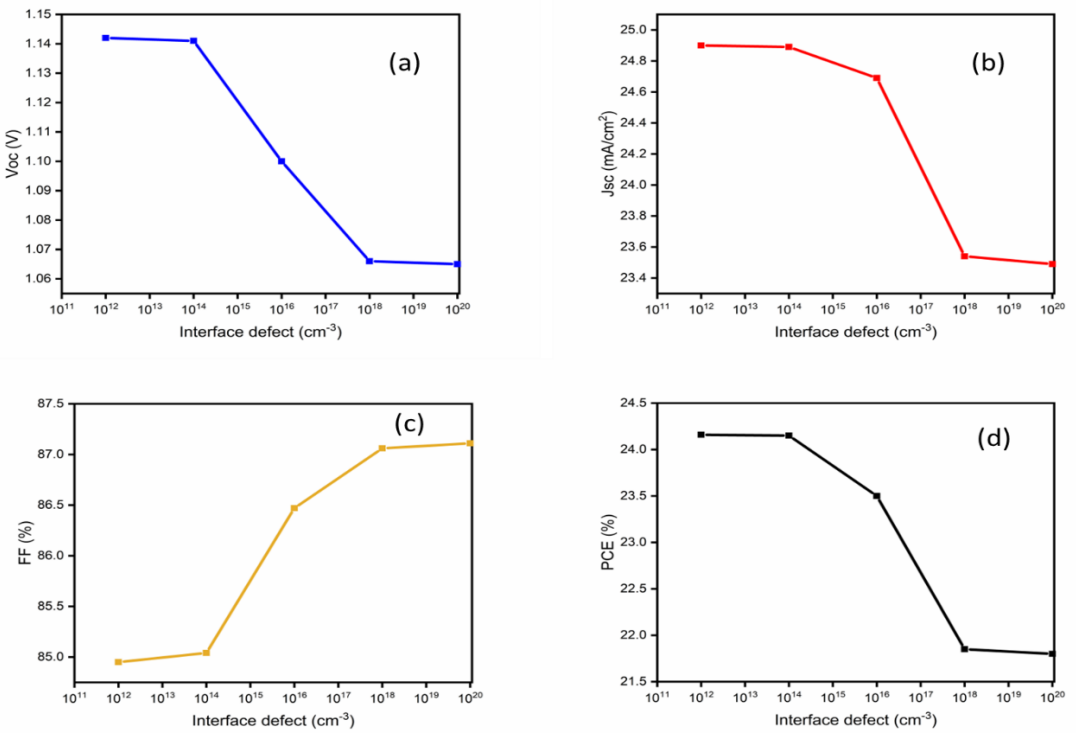

Figure 3: Absorber/CuSbS$_2$ interface defect

3.3. Effect of Absorber/CuO Interface Defect Density

Table 7 and Figure 4 illustrate the effect of absorber/CuO interface defects on the device performance. The significant deterioration in the performance of the CuO-based device with increasing interface defect density can be attributed to enhanced trap-assisted recombination at the CuO/MASnI$_3$ interface. The increased density of interfacial trap states promotes non-radiative recombination, resulting in shorter carrier lifetimes, reduced quasi-Fermi level splitting, and substantial losses in Voc and PCE. Similar behavior has been widely reported in perovskite solar cells, where interfacial defects act as dominant recombination centers that hinder efficient charge extraction and collection (Luo et al., 2020; Sharma, V. et al., 2018; Sherkar et al., n.d.). Moreover, the FF was reduced due to enhanced carrier entrapment and reduced hole extraction efficiency. The observed deterioration indicates the great sensitivity of CuO surfaces to the development of defects. The decrease of Jsc at high defect density also implies the impeded carrier transit and increased recombination probability before charge collection via interface states.

CuO as one of the most promising inorganic HTLs has outstanding stability and p-type conductivity. However, poor interface quality may result in undesirable band offsets and increased interface recombination. The improvement of CuO-based PSC performances is an important aspect of interface engineering and defect passivation, as observed in several research(Luo et al., 2020; Sherkar et al., n.d.; Stolterfoht et al., 2018). Thus, the poor defect tolerance of CuO could be attributed to the unfavourable band alignment and high interface

recombination rates. Therefore, further interface passivation approaches are necessary to enhance the performance of CuO-based tin perovskite solar cells.

Table 7: FTO/WS2/Sn/CuO/Au

S/N	HTL/AL interface defect density (cm^{-3})	Voc(V)	Jsc (A/cm^2)	FF (%)	PCE (%)
1	10^{12}	0.952	25.87	79.50	19.59
2	10^{14}	0.746	25.86	82.77	15.96
3	10^{16}	0.630	25.27	78.84	12.55
4	10^{18}	0.609	23.44	78.90	11.27
5	10^{20}	0.609	23.42	78.92	11.26

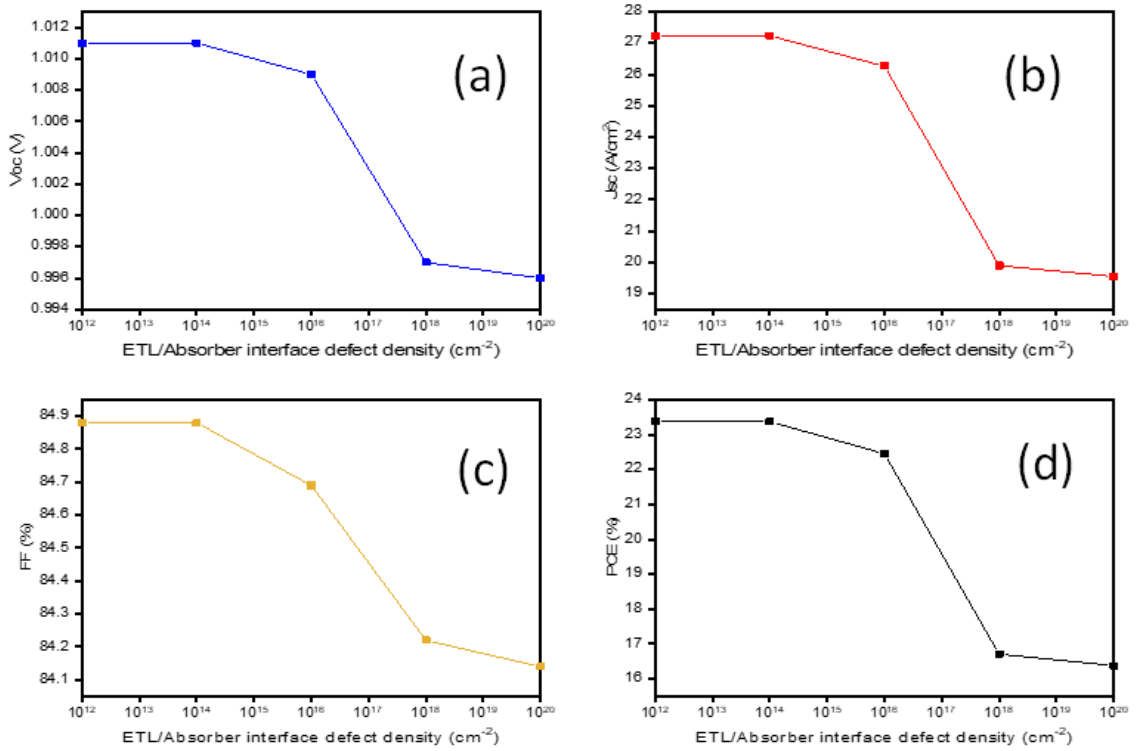

Figure 4: Absorber/CuO interface defect

3.4. Effect of Absorber/Cu_2O Interface Defect Density

The photovoltaic properties of the FTO/WS_2/$MASnI_3$/Cu_2O/Au structure are shown in Table 8 and Figure 5. The device obtained the highest efficiency of 19.25% at the interface defect density of 10^{12} cm^{-3}. However, the efficiency declined gradually to 13.47% at 10^{20} cm^{-3}. The decrease of Voc and FF with increasing defect density suggests that trap-assisted recombination at the absorber/Cu_2O interface is enhanced. Interface defects create localized states in the forbidden bandgap that lead to non-radiative recombination and a corresponding decrease in carrier extraction efficiency. Similar results have been published for SCAPS-based studies of inorganic HTLs for perovskite solar cells. The reduction of FF from 86.18% to 82.00% indicates the increased resistance of carrier transport due to the scattering by defects (Sharma, V. et al., 2018; Sherkar et al., n.d.). Similarly, the modest decrease in Jsc indicates that the interface defects hinder the charge transport across the heterojunction and cause an increase in the carrier losses.

However, the performance decrease was comparatively small for Cu_2O compared to CuO and CuI. This phenomenon can be attributed to its better energy alignment, higher hole mobility and reduced recombination velocity at the absorber contact. Cu_2O has been widely studied as

an eco-friendly HTL for its good optical transparency, high conductivity and steady electrical characteristics. The obtained results demonstrate moderate defect tolerance of Cu_2O and viability as an HTL for TPSCs with appropriate interface passivation techniques (Zuo & Ding, 2015).

Table 8: FTO/WS_2/Sn/ Cu_2O /Au

S/N	HTL/$MASnI_3$ defect density (cm^{-2})	Voc (V)	Jsc (A/cm^2)	FF (%)	PCE (%)
1	10^{12}	0.946	23.63	86.18	19.25
2	10^{14}	0.820	23.62	85.74	16.61
3	10^{16}	0.720	23.58	83.24	14.13
4	10^{18}	0.701	23.44	82.01	13.49
5	10^{20}	0.701	23.44	82.00	13.47

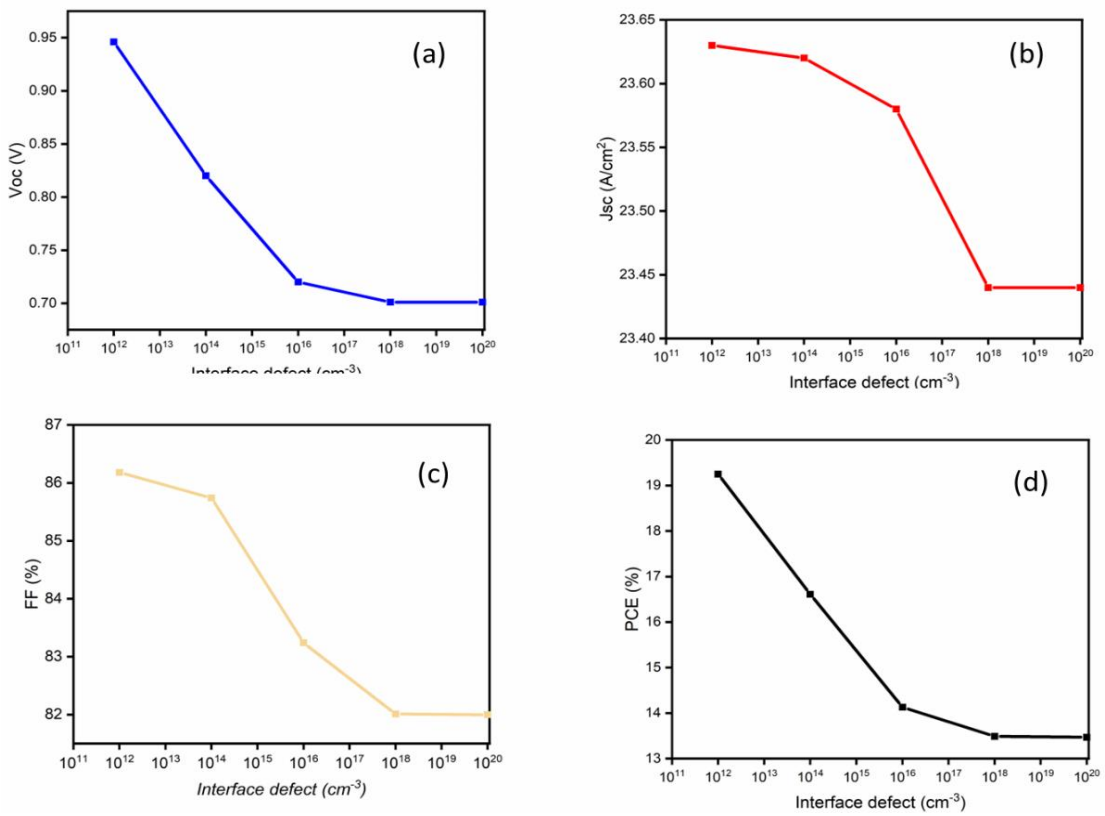

Figure 5: Variation of photovoltaic parameters with absorber/Cu_2O interface defect density

3.5. Effect of Absorber/$CuAlO_2$ Interface Defect Density

The influence of interface defect density on the FTO/WS_2/$MASnI_3$/$CuAlO_2$/Au device design is demonstrated in Table 9 and Figure 6. $CuAlO_2$ showed very good stability to the variation of interface defects. It exhibited the best defect tolerance of all the HTLs used in these studies with only 3% decrease in the efficiency over the entire range of defect variation. The efficiency was almost unchanged as the defect density increased from 10^{12} to 10^{20} cm^{-3}, reducing slightly from 22.83% to 22.66%. The stability of the photovoltaic parameters indicates the excellent defect tolerant property of the $CuAlO_2$ surface. The Voc stayed over 1.11 V for all defect densities and FF climbed marginally from 84.94% to 86.14%. This behavior demonstrates reduced interface recombination and efficient charge extraction at even high defect densities.

It is attributed to good energy band matching, low interface trap formation likelihood and great optical transparency of $CuAlO_2$ for better interface stability. $CuAlO_2$ has been previously shown to possess good electrical conductivity, high transparency and chemical stability, and is hence an interesting HTL material for optoelectronic applications. In addition, the minor variation of Jsc with increasing defect density suggests that $CuAlO_2$ is successful in maintaining the carrier transport across the heterointerface. This pattern supports the reduced trap-assisted recombination and efficient hole selectivity at $CuAlO_2$/$MASnI_3$ contact. The obtained results are confirming that $CuAlO_2$ is one of the most promising inorganic HTLs for stable and high-performance TPSCs (Minemoto & Murata, 2015; Stolterfoht et al., 2018).

Table 9: FTO/WS2/$MASnI_3$/ $CuAlO_2$/Au

S/N	HTL/Absorber Interface defect density (cm^{-3})	Voc(V)	Jsc (A/cm^2)	FF (%)	PCE (%)
1	10^{12}	1.141	23.55	84.94	22.83
2	10^{14}	1.141	23.55	84.94	22.83
3	10^{16}	1.141	23.55	84.98	22.83
4	10^{18}	1.123	23.54	85.89	22.72
5	10^{20}	1.118	23.55	86.14	22.66

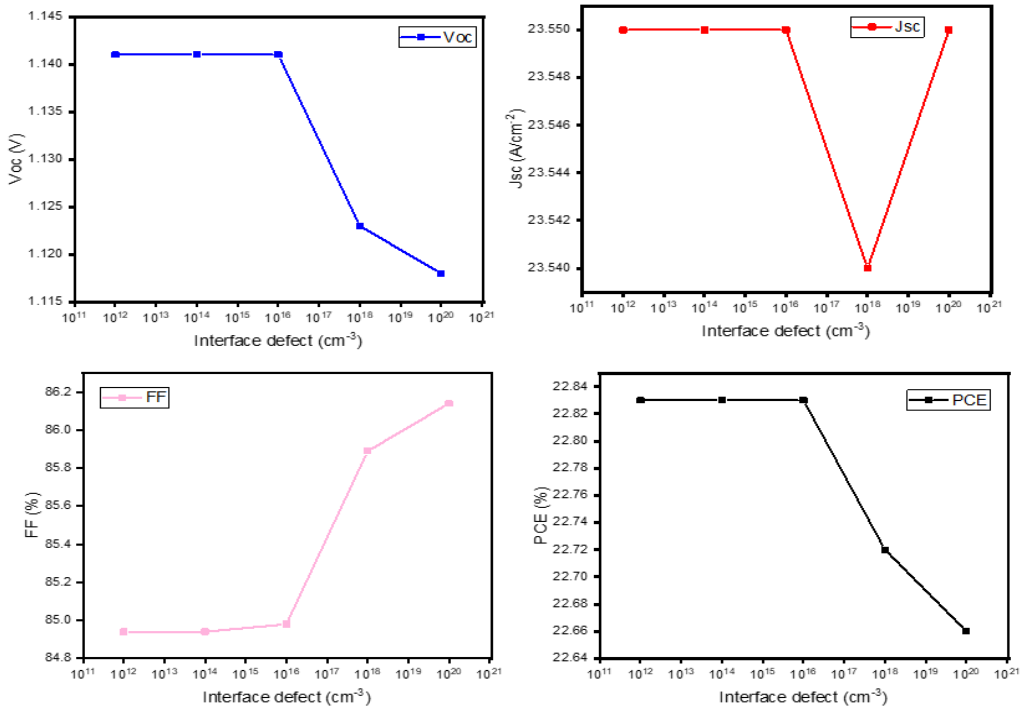

Figure 6: Variation of photovoltaic parameters with absorber/$CuAlO_2$ interface defect density

3.6. Effect of Absorber Layer Defect Density

The effect of the bulk absorber defect density on the photovoltaic performance of the FTO/WS_2/$MASnI_3$/Cu_2O/Au architecture is reported in Table 10 and Figure 7. The results show a significant decrease in the device performance with increase in the bulk defect density. At the defect density of 10^{15} cm^{-3}, the device showed a PCE of 19.25%. However, the efficiency declined dramatically to only 0.04% at 10^{20} cm^{-3}. The considerable drop of Voc, Jsc and FF indicates the deleterious effect of bulk recombination on carrier transportation and extraction. The decrease in Voc from 0.946 V to 0.462 V is mainly related to the increased trap states in the absorber layer resulting in the enhanced SRH recombination. Bulk defects in tin-based perovskites are known to occur from vacancies, interstitials and oxidation related

defects due to oxidation of Sn^{2+} to Sn4+. Such defects introduce deep trap states that promote non-radiative recombination and reduce carrier lifespan.

Similarly, the sharp drop of Jsc implies serious trap of carrier and less diffusion length. In previous investigations, it was revealed that high bulk defect density affects carrier mobility and raises the recombination likelihood before carrier collection, which greatly decreases the device efficiency. The drastic fall of FF from 86.18% to 22.35% further implies the higher series resistance and poor charge transport due to defect-induced scattering mechanisms. These results indicate that the reduction of bulk defects in tin-based perovskite absorbers is crucial to achieve good device performance. Thus, appropriate passivation procedures, additive engineering and controlled fabrication techniques are required to minimize trap formation, improve crystal quality and boost operational stability of tin-based PSCs.

Table 10: Absorber layer defect density of FTO/WS_2/$MASnI_3$/ Cu_2O /Au Architecture

S/N	AL defect density (cm^{-3})	Voc(V)	Jsc (A/cm^2)	FF (%)	PCE (%)
1	10^{15}	0.946	23.62	86.18	19.25
2	10^{16}	0.938	23.55	80.51	17.79
3	10^{17}	0.909	22.89	57.02	11.86
4	10^{18}	0.850	17.44	30.30	4.49
5	10^{19}	0.583	3.18	22.35	0.41
6	10^{20}	0.462	0.30	26.69	0.04

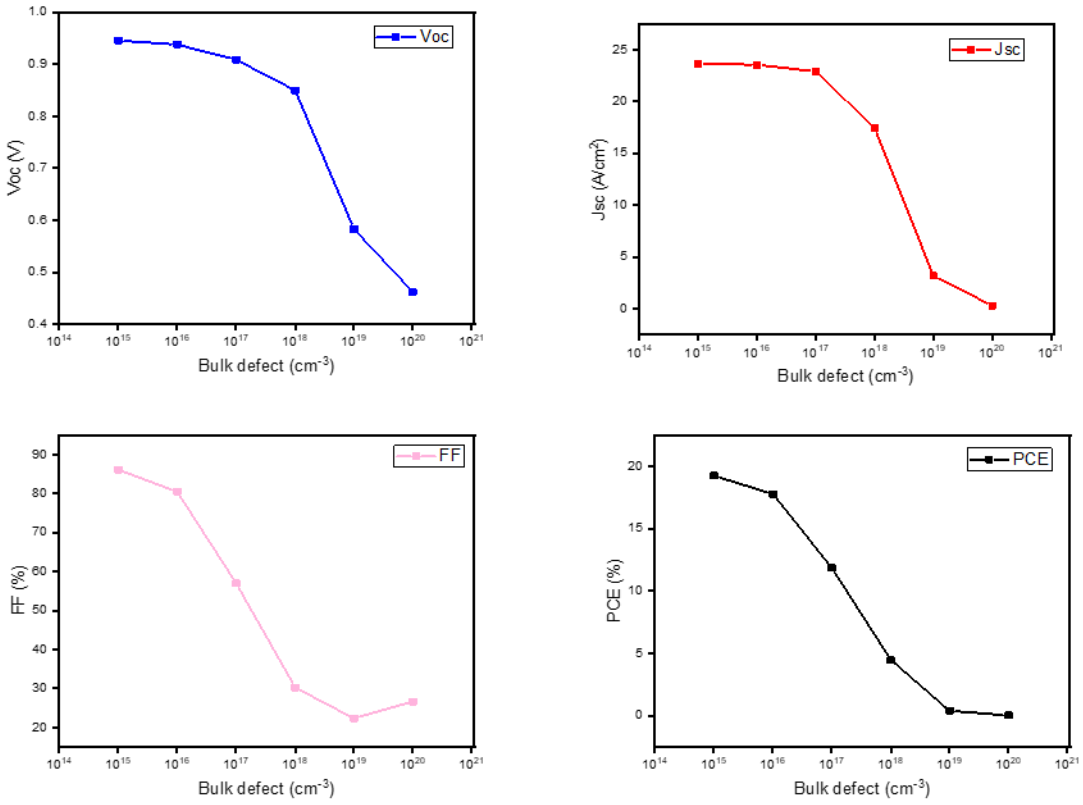

Figure 7: Influence of absorber layer defect density on photovoltaic performance

3.7. Effect of Absorber/ETL Interface Defect Density

The effect of the absorber/ETL interface defect density on FTO/WS_2/Sn/CuI/Au structure is shown in Table 11 and Figure 8. The results show that the device performance degrades remarkably with the increase of the interface defect density. The PCE dropped from 15.47% at 10^{12} cm^{-2} to 9.78% at 10^{20} cm^{-2}. Voc droped from 0.779 V to 0.533 V, suggesting an increase in interface recombination losses at the ETL/absorber interface. The decrease of Voc is well

consistent with earlier works showing that the presence of ETL/perovskite interface defects facilitates the non-radiative recombination and reduces the carrier extraction efficiency.
The decrease in FF and Jsc further confirms that the interface traps are detrimental to the electron extraction and lead to charge carrier recombination. The defect states at the ETL/perovskite interface can serve as recombination centers to trap the photogenerated electrons before they are transferred to the external circuit. Moreover, a rise in defect density can lead to undesirable band bending and spatial electric field fluctuations, which can decrease the efficiency of charge separation. Similar observations have been reported for inorganic electron transport layers in perovskite solar cells where interface passivation has been shown to greatly improve the stability and efficiency of the device. These results emphasize the necessity of designing ETL/absorber interfaces to avoid recombination and enhance device efficiency. Therefore, high-performance lead-free TPSCs require efficient interface passivation and defect reduction methods.

Table 11: FTO/WS2/MASnI$_3$/CuI/Au

S/N	Absorber/ETL Interface defect density (cm^{-2})	Voc(V)	Jsc (A/cm^2)	FF (%)	PCE (%)
1	10^{12}	0.779	23.64	83.97	15.47
2	10^{14}	0.652	23.64	83.19	12.82
3	10^{16}	0.551	23.58	79.87	10.38
4	10^{18}	0.533	23.42	78.41	9.79
5	10^{20}	0.533	23.41	78.39	9.78

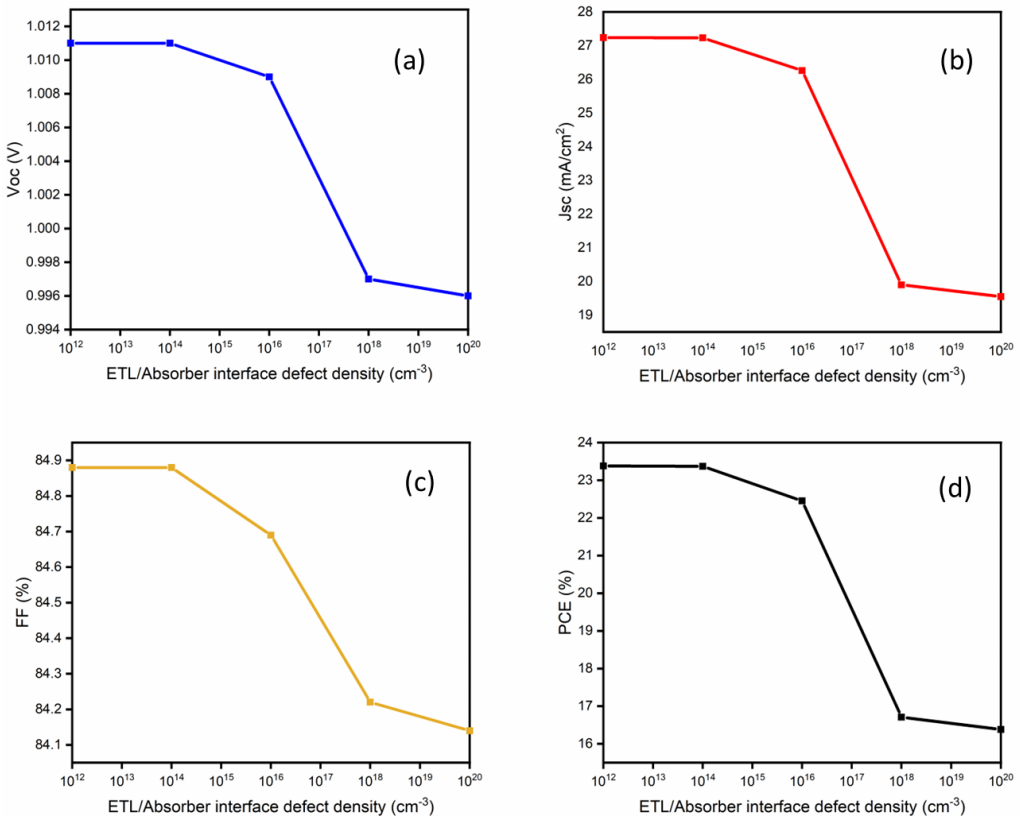

Figure 8: Variation of photovoltaic parameters with absorber/ETL interface defect density

3.8. Comparative Analysis of HTLs

The comparative analysis of the examined HTLs shows the best defect tolerance and overall photovoltaic performance are $CuSbS_2$ and $CuAlO_2$. $CuSbS_2$ obtained the maximum efficiency

of 24.16%. $CuAlO_2$ obtained the highest interface stability to defect change with of 3% decrease in the efficiency over the entire range of defect densities variation. MoS_2 likewise showed relatively high efficiency but was more sensitive to contact defects than $CuSbS_2$ and $CuAlO_2$. On the other hand, CuO showed poor defect tolerance and large performance deterioration at high defect densities. The better performance of $CuSbS_2$ and $CuAlO_2$ can be due to the favorable energy level alignment, low interface recombination velocity and effective hole extraction. These materials are promising HTLs for next-generation lead-free tin perovskite solar cells.

Table 12: Values of CBO and VBO for the hole transport materials used

HTL	VBO (eV)	CBO (eV)	Expected Performance
MoS_2	+0.01	0.00	Excellent
$CuSbS_2$	-0.28	0.00	Excellent
$CuAlO_2$	-0.46	+1.70	Excellent defect tolerance
CuO	-0.08	+0.13	Moderate
Cu_2O	+0.13	+1.00	Moderate
CuI	+0.40	+2.10	Less favorable

4.0. CONCLUSION

The simulation analysis of interface and bulk defects in tin-based perovskite solar cells using SCAPS-1D was successfully performed in a comprehensive manner. We extensively examined the effects of defects at absorber/HTL interface, absorber/ETL interface and absorber bulk on the photovoltaic performance. The results show that interface defects greatly affect the carrier recombination, charge extraction and device efficiency. $CuSbS_2$ displayed the best efficiency of 24.16% with a great defect tolerance, it is the second-best defect tolerance of all the studied HTLs with only about 10% decrease in PCE from 10^{12}-10^{20} cm^{-3} range of defect densities. $CuAlO_2$ on the other hand exhibited the best interfacial interface stability with low efficiency deterioration over a wide range of defect densities, the PCE only decrease by 3% over the entire range of defect densities.

Analysis of the bulk defects of the absorber indicated that the performance of the device is severely degraded at high defect concentrations due to the accelerated Shockley-Read-Hall recombination. Furthermore, defects at the ETL/absorber interface drastically decreased the device performance owing to the enhanced recombination loss. In a nutshell, the study proves that interface engineering and defect passivation are efficient ways to improve the efficiency and operational stability of lead-free Sn-based perovskite solar cells. The findings provide useful guidance for the experimental creation of high-performance eco-friendly PSCs.

ACKNOWLEDGEMENT

The authors acknowledge the use of SCAPS-1D simulation software developed by the Department of Electronics and Information Systems (ELIS), University of Ghent, Belgium.

REFERENCES

Ain, N., Malek, A., Alias, N., Khatijah, S., Adliha, N., Zhang, X., Li, X., Shi, Z., Mustaqim, M., Hasnan, T., Abd, T., Ali, A., & Zhan, Y. (2020). Ultra-thin MoS 2 nanosheet for electron transport layer of perovskite solar cells. *Optical Materials*, *104*(April). https://doi.org/10.1016/j.optmat.2020.109933

Asif, P., Chetia, A., Saikia, D., & Sahu, S. (2025). A comprehensive theoretical investigation of lead-free mixed antimony-bismuth halide double perovskite ($Cs_2AgBi_{0.75}Sb_{0.25}Br_6$) solar cell using SCAPS-1D. *Discover Electronics*, *2*(1). https://doi.org/10.1007/s44291-025-00085-8

Atem, M. Al, & Makableh, Y. (2025). Towards Sustainable Perovskite Solar Cells : Lead-Free High Efficiency Designs with Tin and Germanium. *Eng MDPI*, *6*(38).

Bhujbal, P. K., Sakunde, B. M., Supekar, A. T., Bhandari, H. M., Saini, S., & Dhirhe, D. (2024). Unlocking the Potential of WS 2 as an Electron Transport Layer in Flexible and Lead-Free Methylammonium Tin Iodide-Based Perovskite Solar Cells : A Comprehensive Defect Study Using the SCAPS-1D Framework. *ES Energy and Environment*, *26*, 1–10. https://doi.org/https://dx.doi.org/10.30919/esee1225

Chalapathi, U., Bhaskar, P. U., Sangaraju, S., Al-asbahi, B. A., & Park, S. (2024). CuSbS2 thin films and solar cells produced from Cu/ Sb/Cu stacks via sulfurization. *Heliyon*, *10*(6), e27504. https://doi.org/10.1016/j.heliyon.2024.e27504

D, K., Y, C., U, K., J, K., J, S., E, S., H, M., J, K., & H., P. (2025). Mesoporous structured MoS2 as an electron transport layer for efficient and stable perovskite solar cells. *National Nanotechnology*, *20*(1), 75–82. https://doi.org/doi: 10.1038/s41565-024-01799-8.

He, Y., Xu, L., Yang, C., Guo, X., & Li, S. (2021). Design and Numerical Investigation of a Lead-Free Inorganic Layered Double Perovskite Cs 4 CuSb 2 Cl 12 Nanocrystal Solar Cell by SCAPS-1D. *Nanomaterials*, *11*, 1–19. https://doi.org//doi.org/10.3390/nano11092321

Islam, B., Khan, T. M., Rahaman, M. M., & Al Ahmed, S. R. Al. (2026). Computational optimization of MASnI3 perovskite solar cells using SCAPS-1D simulations and machine learning techniques. *RSC Advances*, *2*, 1172–1192. https://doi.org/10.1039/d5ra07200j

Javed, A., Farooq, M., Qasim, I., Mohammed, Y., & Tahir, M. (2024). International Journal of Electrochemical Science Numerical modelling of an effective perovskite solar cell and PV-module for comparison analysis of organic and inorganic electron transport layers. *International Journal of Electrochemical Science*, *19*(8), 100641. https://doi.org/10.1016/j.ijoes.2024.100641

Kim, H. S., Lee, C. R., Im, J. H., Lee, K. B., Moehl, T., Marchioro, A., Moon, S. J., Humphry-Baker, R., Yum, J. H., Moser, J. E., Grätzel, M., & Park, N. G. (2012). Lead iodide perovskite sensitized all-solid-state submicron thin film mesoscopic solar cell with efficiency exceeding 9%. *Scientific Reports*, *2*, 1–7. https://doi.org/10.1038/srep00591

Lee, M. M., Teuscher, J., Miyasaka, T., Murakami, T. N., & Snaith, and H. J. (2012). Efficient Hybrid Solar Cells Based on Meso-Superstructured Organometal Halide Perovskites. *Science*, *338*(6107), . 643-647. https://doi.org/10.1126/science.122860

Li, P., Cao, X., Li, J., Jiao, B., Hou, X., Hao, F., Ning, Z., Bian, Z., Xi, J., Ding, L., Wu, Z., & Dong, H. (2023). Ligand Engineering in Tin - Based Perovskite Solar. In *Nano-Micro Letters* (Vol. 15, Issue 1). Springer Nature Singapore. https://doi.org/10.1007/s40820-023-01143-0

Luo, D., Su, R., Zhang, W., Gong, Q., & Zhu, R. (2020). Minimizing non-radiative recombination losses in perovskite solar cells. *Nature Reviews Materials*, *5*(1), 44–60. https://doi.org/doi.org/10.1038/s41578-019-0151-y

Minemoto, T., & Murata, M. (2015). Device Modeling of Perovskite Solar Cells Based on Structural Similarity with Thin Film Inorganic Semiconductor Solar Cells. *Journal of Applied Physics*, *116*. https://doi.org/10.1063/1.4891982

Mortadi, A., El Hafidi, E., Nasrellah, H., Monkade, M., & El Moznine, R. (2024). Analysis and optimization of lead-free perovskite solar cells: investigating performance and electrical characteristics. *Materials for Renewable and Sustainable Energy*, *13*(2), 219–232. https://doi.org/10.1007/s40243-024-00260-z

National Renewable Energy Laboratory (NREL). (2025). *Best research-cell efficiency chart.*

Obi, U. C., Sanni, D. M., & Bello, A. (2021). Effect of Absorber Layer Thickness on the Performance of Bismuth-Based Perovskite Solar Cells. *Semiconductors*, *55*(12), 922–927. https://doi.org/10.1134/S1063782621040114

Pau, R., Romero, G., Pitaro, M., Feng, Q., Loi, M. A., & Mario, L. Di. (2025). Solution-processed CuI as a hole transport layer for Sn – Pb perovskite solar cells. *Journal of Materials Chemistry A*, *13*, 42118–42127. https://doi.org/10.1039/d5ta06770g

Rachidy C., B., H., S., T., S., M., A., F., F., B., M., E., S., F., M., S., P., T., & A., H. (2021). Enhancing CZTS solar cell parameters using CZTSe BSF layer and nontoxic SnS2/In2S3 buffer layer. *4th International Conference on Advanced Materials for Photonics, Sensing and Energy Conversion Energy Applications (AMPSECA), Marrakech, Morocco*, 26–36. https://doi.org/10.1016/j.matpr.2022.03.106

Sharma, V., Kumar, A., Sastry, O. S., & Dwivedi, P. K. (2018). Effect of interface defect density on performance of perovskite solar cell: Correlation of simulation and experiment. *Materials Letters*, 150–153. https://doi.org/doi.org/10.1016/j.matlet.2018.03.095

Shasti, M. and Mortezaali, A. (2019). Numerical Study of Cu2O, SrCu2O2, and CuAlO2 as Hole-Transport Materials for Application in Perovskite Solar Cells. *Physics Status Solidi*, *216*. https://doi.org/https://doi.org/10.1002/pssa.201900337

Sherkar, T. S., Momblona, C., Gil-Escrig, L., Ávila, J., Sessolo, M., & Bolink, H. J. (n.d.). Recombination in Perovskite Solar Cells: Significance of Grain Boundaries, Interface Traps, and Defect Ions. *ACS Energy Letters*, *2*(5), 1214–1222. https://doi.org/https://doi.org/10.1021/acsenergylett.7b00236

Sobayel, K., Rahman, K. S., Ferdaous, M. T., & Al-mutairi, Z. A. (2019). A comprehensive defect study of tungsten disul fi de (WS2) as electron transport layer in perovskite solar cells by numerical simulation. *Results in Physics*, *12*(December 2018), 1097–1103. https://doi.org/10.1016/j.rinp.2018.12.049

Stolterfoht, M., Wolff, C. M., Márquez, J. A., Zhang, S., Hages, C. J., Rothhardt, D., Albrecht, S., Burn, P. L., Meredith, P., Unold, T., & Neher, D. (2018). Visualization and suppression of interfacial recombination for high-efficiency large-area pin perovskite solar cells. *Nature Energy*, *3*(10), 847–854. https://doi.org/doi.org/10.1038/s41560-018-0219-8

Stranks, S. D., Eperon, G. E., Grancini, G., Menelaou, C., & Snaith, H. J. (2013). Electron-Hole Diffusion Lengths Exceeding Trihalide Perovskite Absorber. *Science*, *342*(October), 341–344. https://doi.org/10.1126/science.1243982

Wang, S., & Xiu, H. (2025). Recent Advances in the Structure , Properties , and Applications of Lead - Free Tin - Based Perovskites in Optoelectronic Devices. *World Scientific Research Journal*, *11*(4), 133–146. https://doi.org/10.6911/WSRJ.202504

Wang, X., Yang, J., Zhong, J., & Yu, J. (2024). Innovative Materials for High-Performance Tin-Based Perovskite Solar Cells : A Review. *Polymers*, *16*, 1–18. https://doi.org/doi.org/10.3390/polym16213053

Willian, F., Lucas, D. S., Welch, A. W., Baranowski, L. L., Dippo, P. C., Hempel, H., Unold, T., Eichberger, R., Blank, B., Rau, U., Mascaro, L. H., & Zakutayev, A. (2016). Effects of Thermochemical Treatment on CuSbS2 Photovoltaic Absorber Quality and Solar Cell Reproducibility. *Journal of Physicsal Chemistry C*, *3*, 18377−18385. https://doi.org/10.1021/acs.jpcc.6b04206

Zhang, B., Zeng, Z., Dong, H., & Ran, C. (2025). Recent advances in tin halide perovskite solar cells : *Journal of Materials Chemistry A*, *13*, 30708–30754. https://doi.org/10.1039/d5ta04568a

Zuo, C., & Ding, L. (2015). Solution-Processed Cu2O and CuO as Hole Transport Materials for Efficient Perovskite Solar Cells. *Small*, *11*(41), 5528–5532. https://doi.org/10.1002/smll.201501330.